Supporting Information for

Magnetic Fano resonance-induced second-harmonic generation enhancement in plasmonic metamolecule rings †

Da-Jie Yang,[a,b] Song-Jin Im,*[c] Gui-Ming Pan,[b] Si-Jing Ding,[b] Zhong-Jian Yang,[a,d] Zhong-Hua Hao,[b] Li Zhou,*[b] and Qu-Quan Wang*[a,b]

[a.] *The Institute for Advanced Studies, Wuhan University, Wuhan 430072, P. R. China. E-mail: qqwang@whu.edu.cn,*

[b.] *Key Laboratory of Artificial Micro- and Nano-structures of the Ministry of Education and School of Physics and Technology, Wuhan University, Wuhan 430072, P. R. China. E-mail: zhouli@whu.edu.cn,*

[c.] *Department of Physics, Kim Il Sung University, Pyongyang, Democratic People's Republic of Korea. email: ryongnam7@yahoo.com.*

[d.] *Hunan Key Laboratory of Super Microstructure and Ultrafast Process, School of Physics and Electronics, Central South University, Changsha, Hunan 410083, P.R. China*

The influence of the absorption

While Fano resonances will lead to strongly asymmetric scattering spectra, Fano resonances can't be observed in the absorption spectra of the oligomer structures. But there will usually be an absorption peak at the subradiant mode.[1,2] The nanostructure gets energy from the light through absorption and the energy is stored as the plasmonic energy.[3] The plasmonic energy will undergo radiative losses and nonradiative losses.[3] The radiative losses are related to the scattering of the nanoparticles. Since it harvests more energy at the absorption peak than other frequency, it is necessary to compare the SHG corresponding to the Fano dip with that corresponding to the absorption peak. Because the scattering dip and absorption peak of the trimer with r_1 = 125 nm are not corresponding to the same wavelength as shown in Fig. S6, this structure is chosen to be further studied in Fig. S7. The comparison of the scattering dip and the absorption peak at different wavelengths will further prove the advantage of the magnetic Fano dip in enhancing SHG.

The scattering and absorption cross sections are shown in Fig. S7a and Fig. S7b respectively. The scattering dip is denoted by the yellow bar and the absorption peak is denoted by the green bar. The scattering cross section at the green bar is about 2.9 times that at the yellow bar, while the

absorption cross section at the green bar is about 1.4 times that at the yellow bar. Fig. S7c shows the electric near fields at the scattering dip (left) and absorption peak (right). The electric on the right is a little stronger than that on the left. The strong electric near field is mainly determined by the energy absorption and dissipation. The right one harvest more energy than the left one. At the same time, the right one suffers more radiative losses. But the SHG near field in Fig. 7d and the SHG far field in Fig. 7e corresponding to the absorption peak are weaker than the Fano dip. There seems two reason. Firstly, at the particle surface where the centrosymmetry is broken, the surface-perpendicular components of the near field is stronger for the scattering dip than that for the absorption peak as shown in Fig. S8, although the absorption peak produces stronger near field at the three gaps. The stronger surface-perpendicular components of the near field at the magnetic Fano dip is attributed to the ring current mode. Secondly, at the scattering dip, even with smaller absorption, the trimer suffers the minimum radiative losses and the influence of the radiative losses on SHG may be stronger than on the fundamental electric near field. By this conclusion, we don't deny that on some specified conditions the absorption peak will produce stronger SHG signal. But in our case, the magnetic mode and electric quadrupole mode cause vary small energy radiation, so the strongest SHG happens with the excitation at the magnetic Fano dip.

SHG of nanostructures without Fano resonance

As another evidence to show the superiorities of the magnetic Fano resonance, the fundamental and harmonic behaviors of two dimers (without Fano resonance) — small-small dimer and big-small dimer — are compared with the fundamental and harmonic behaviors of the trimer. In the scattering spectra in Fig. S9a, the small-small dimer and the big-small dimer show obvious longitudinal modes at about 745 nm and 1160 nm respectively. The excitation wavelengths are denoted by the triangular symbols. We compare the SHG of the trimer with the two dimers. The trimer shows the largest SHG enhancement for both the near field Fig. S9b and the far field Fig. S9c, and the enhancement of the SHG far field is especially obvious. This is because the two dimers possess large electric dipole moments, which means the fundamental radiation losses is relatively strong, and at the trimer scattering dip the magnetic Fano resonance reduces radiative losses in the trimer structure.

Comparison of the scattering dip and the absorption dip in the structure with electric Fano resonance

The wavelengths corresponding to the minima of absorption and scattering are different as shown in Fig. 4a. Compared with the extinction dip at 650 nm, the absorption at 625 nm becomes stronger, the scattering become weaker (see Fig. 4a), so the fundamental and the second harmonic near fields become a little stronger (see Fig. S14). And the fundamental and second harmonic near fields at 625 nm (scattering dip) are still weaker than those at the two absorption peaks at 610 and 695 nm. This result does not in contradictory with Fig. S7. In Fig. S14 for electric Fano, the absorption efficiency at the absorption peaks is much larger than that at the scattering dip (625 nm), then the stronger optical response occurs at the absorption peaks. In Fig. S7 for magnetic Fano, the scattering efficiency at the scattering dip is much lower than that at the absorption peak, then the stronger optical response occurs at the scattering dip. Maybe we can rank the optical response strengths: 1st magnetic Fano dip (weak scattering and strong absorption), 2nd electric "Fano peak" (strong absorption and strong scattering), 3rd electric Fano dip (weak scattering and weak absorption). The ratio of the fundamental near field integration at 610 nm, 625 nm, 650 nm and 695 nm is 1.28:1.19:1:1.46. The ratio of the SHG near field integration at 305 nm, 312.5 nm, 325 nm and 347.5 nm is 2.86:1.71:1:2.88. These results are absolutely consistent with our conclusions.

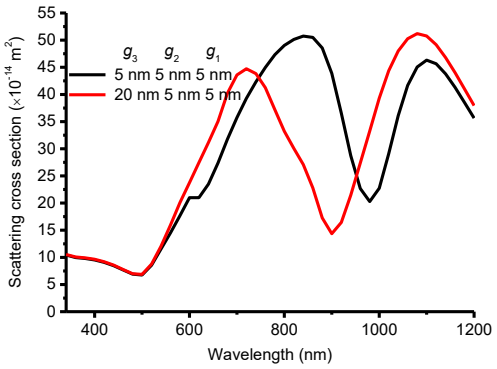

Fig. S1 The scattering cross sections of the trimer with different gaps between the big and small disks (g_1 or g_2). The three disk radii r_1 = 175 nm, r_2 = r_3 = 80 nm. Even with smaller g_3, we can't get deeper Fano dip. This is because it induces symmetry when the three gaps are the same. So it paves the way releasing the restricted small gap size limitation for fabrication.

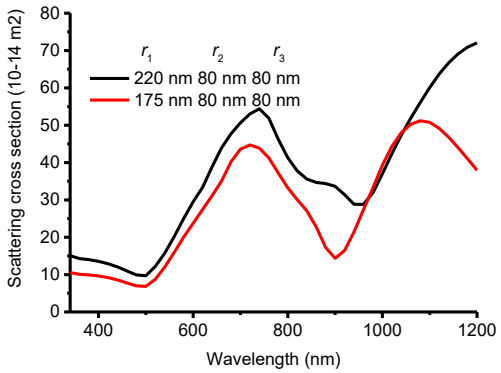

Fig. S2 The scattering cross sections of the trimer with big disk radii r_1 = 220 nm and 175 nm. The three gaps g_1 = g_2 = 5 nm, g_3 = 20 nm. With larger r_1, we can't get deeper Fano dip. When r_1 becomes 220 nm, on the one hand, the dipole moments in the big and small disks become more inequivalent; on another, the overlap of the spectra of the big and small disks become smaller.

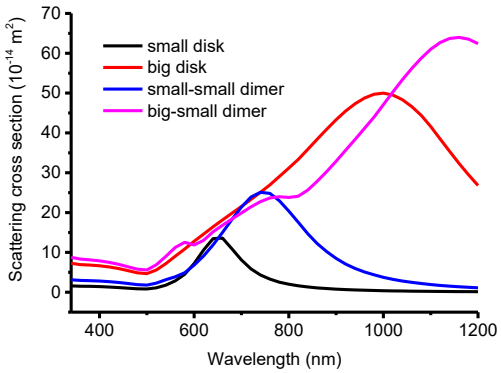

Fig. S3 The scattering cross section of the unit cells in the trimer. The individual small disk (black line), the individual big disk (red line), the small-small disk dimer (blue line) and the big-small disk dimer (pink line) are from the trimer with big disk radius r_1 = 175 nm, small disk radii r_2 = r_3 = 80 nm, small-small dimer gap g_3 = 20 nm, and big-small dimer gap g_1 = 5 nm.

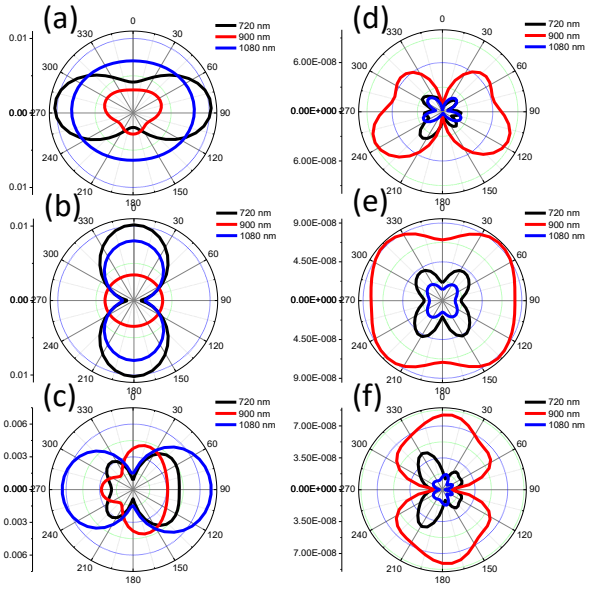

Fig. S4 The fundamental (a-c) and harmonic (d-f) far field with excitation wavelengths of 720 nm (black line), 900 nm (red line) and 1080 nm (blue line) in x = 0 plane (a, d), y = 0 plane (b, e) and z = 0 plane(c, f). For the fundamental response, the minimum far field is found at the Fano dip in each normal. SHG far field corresponding to the Fano dip dominates head and shoulders above those corresponding to the two peaks.

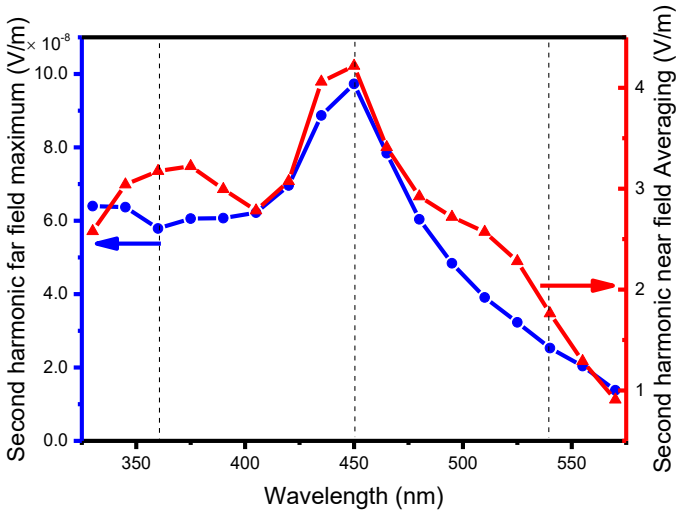

Fig. S5 The SHG efficiency at the whole spectra range. The blue line stand for the maximum value of second harmonic far field collected at any angle. The red line stands for the second harmonic near field averaging in the central plane of the trimer. The area we make the averaging is a circle centered on the three disks. The radium of the circle is 1500 nm. The dash lines from left to right show the wavelengths corresponding to the scattering peak on the high energy side, the magnetic Fano dip and the scattering peak on the low energy side.

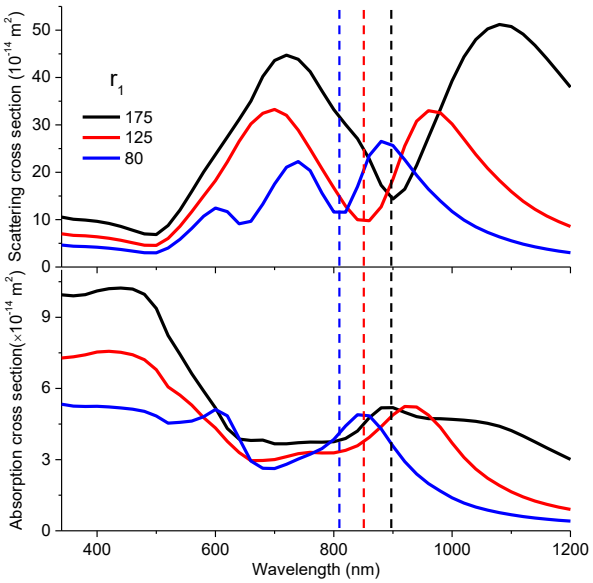

Fig. S6 The comparison of the scattering and absorption cross sections of the trimer with different big disk radii r_1. The three gaps $g_1 = g_2 = 5$ nm, $g_3 = 20$ nm. The small disk radii $r_2 = r_3 = 80$ nm. With $r_1 = 175$ nm, the absorption peak near 900 nm is nearby the scattering peak and the absorption peak near 1050 nm is too broad and unclear. With $r_1 = 80$ nm, the absorption peak is clear but the quadrupolar mode in the big disk disappears. In order to show the generality of the results in the trimer, the scattering dip at 850 nm and the absorption at 930 nm with $r_1 = 125$ nm are chosen to be further studied in Figure 4.

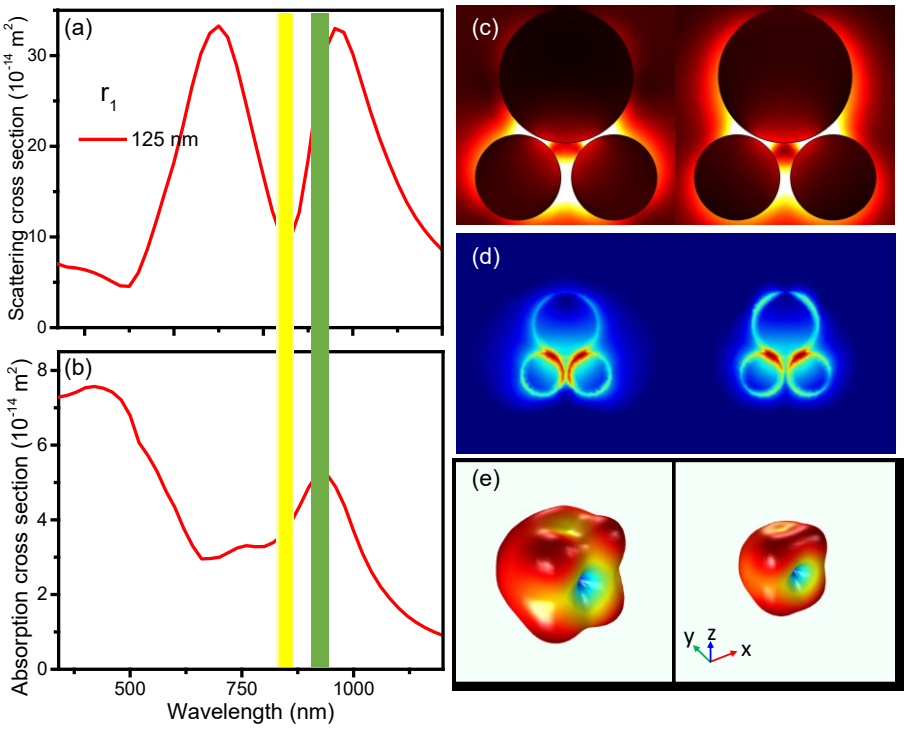

Fig. S7 (a, b) The scattering and absorption cross sections of the trimer structures with the big disk radius of 125 nm. (c) The in-plane electric near field at the fundamental frequency. (d, e) The in-plane electric field and the electric far field at harmonistic frequency respectively. The left column and the right column in (c-e) correspond to the excitation wavelengths of scattering dip and the absorption peak as denoted by the yellow and green bars in (a) and (b) respectively. The harmonic near fields are shown on a logarithmic scale.

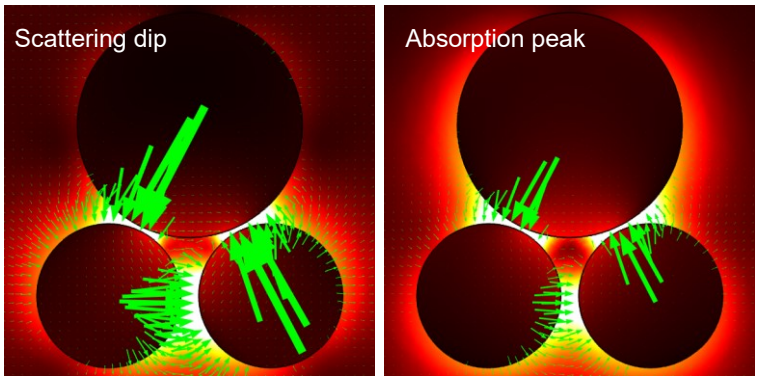

Fig. S8 The electric near field and the surface-perpendicular components at the fundamental frequencies of the scattering dip (left) and the absorption peak (right) of the trimer with the big disk radius of 125 nm. The colors show the near field distribution on the central plane of the trimer. The arrow lengths show the amplitudes of the surface-perpendicular components of the electric near field and the arrow directions show the directions of the surface-perpendicular components of the electric near field at the arrow heads. At the particle surface where the centrosymmetry is broken, the surface-perpendicular components of the near field are stronger for the scattering dip than that for the absorption peak, although the absorption peak produces stronger near field at the three gaps.

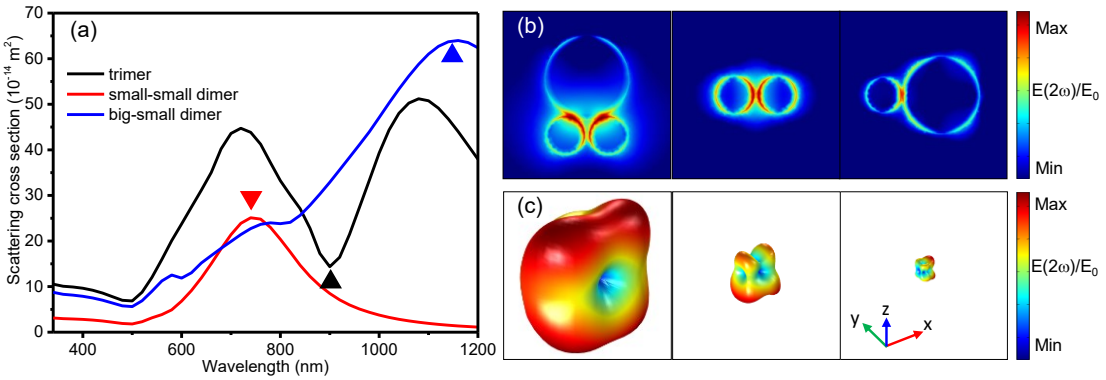

Fig. S9 (a) The scattering cross sectionsof the trimer (black line), small-small dimer (red line) and big-small dimer (blue line). SHG near field (b) and SHG far field (c) are corresponding to the excitation wavelength of the trimer Fano dip, the small-small dimer longitudinal mode and big-small dimer longitudinal mode, respectively. These three excitation positions are denoted by the triangular symbols in (a). The harmonic near fields are shown on a logarithmic scale.

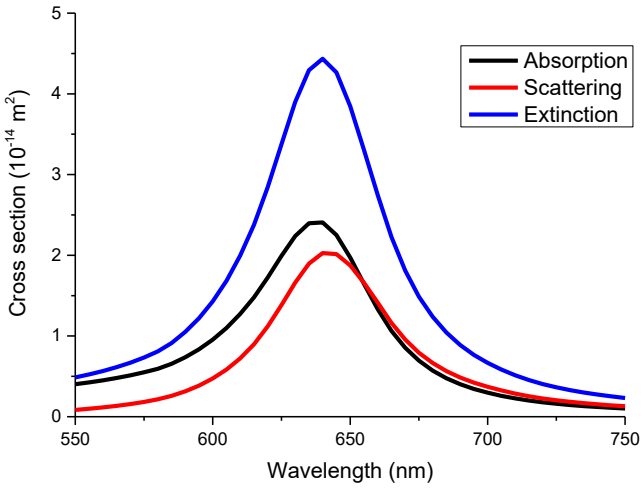

Fig. S10 The absorption (black line), scattering (red line), and extinction (blue line) of the shorter rod in Fig. 4 in the main text. The incident light polarizes along the long axis of the rod.

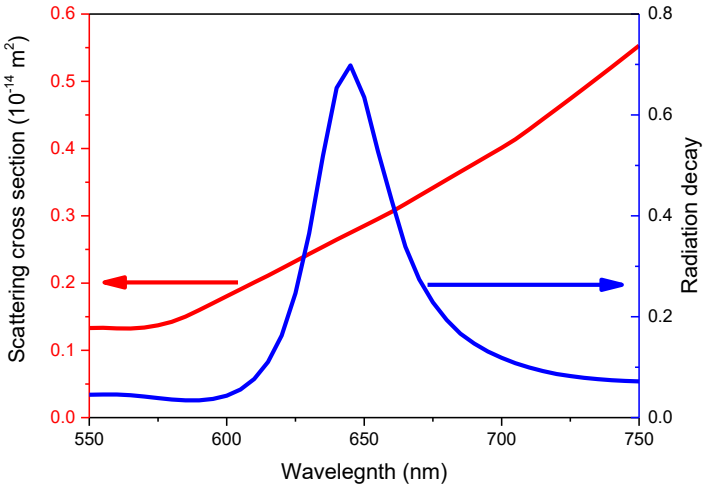

Fig. S11 The scattering (red line), and radiation rate (blue line) of the longer rod in Fig. 4 in the main text. The incident light polarizes along the long axis of the rod. The distance between the dipole source and the rod end is 10 nm. The peak in the radiation spectrum does not appear in the scattering spectra indicate this mode is a dark mode.

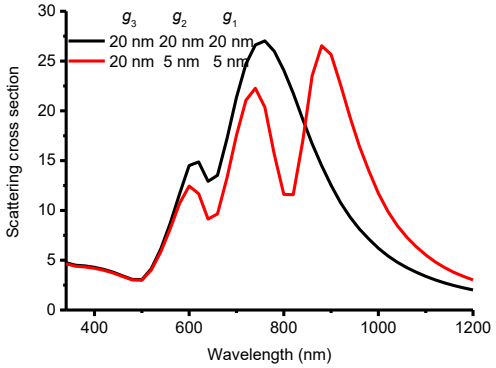

Fig. S12 The scattering cross sections of the trimer with different gaps between the big and small disks (g_1 or g_2). The three disk radii r_1 = r_2 = r_3 = 80 nm. Even when the three disk radii are the same, the trimer with different gaps shows a clear Fano dip. Only on the conditions that all the trimer gaps and the disk radii are the same respectively, will the Fano resonance disappear.

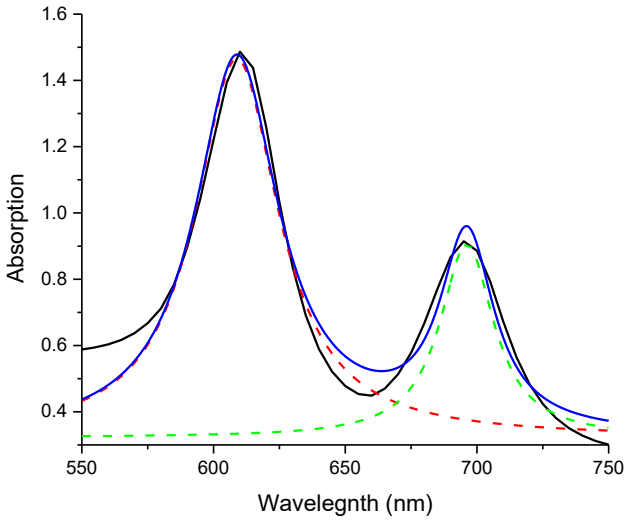

Model	Lorentz		
Equation	y = y0 + (2*A/PI)*(w/(4*(x-xc)^2 + w^2))		
Reduced Chi-Sqr	0.00493		
Adj. R-Squar	0.9483		
		Value	Standard Err
Peak1(B)	y0	0.3223	0.03399
Peak1(B)	xc	608.8601	0.68874
Peak1(B)	w	38.52371	2.89556
Peak1(B)	A	69.23499	5.57995
Peak1(B)	H	1.14414	0.04591
Peak2(B)	y0	0.3223	0.03399
Peak2(B)	xc	696.1636	1.07938
Peak2(B)	w	24.85912	4.15402
Peak2(B)	A	22.83978	3.73021
Peak2(B)	H	0.58491	0.05289

Fig. S13 Fitting of absorption cross section for the nanostructure supporting electric Fano resonance. The black solid line stands for the simulated result, the blue solid line stands for the fitting result, and the red and green dash lines stand for the two Lorentz profiles for fitting the absorption. Two absorption peaks are somewhat asymmetric.

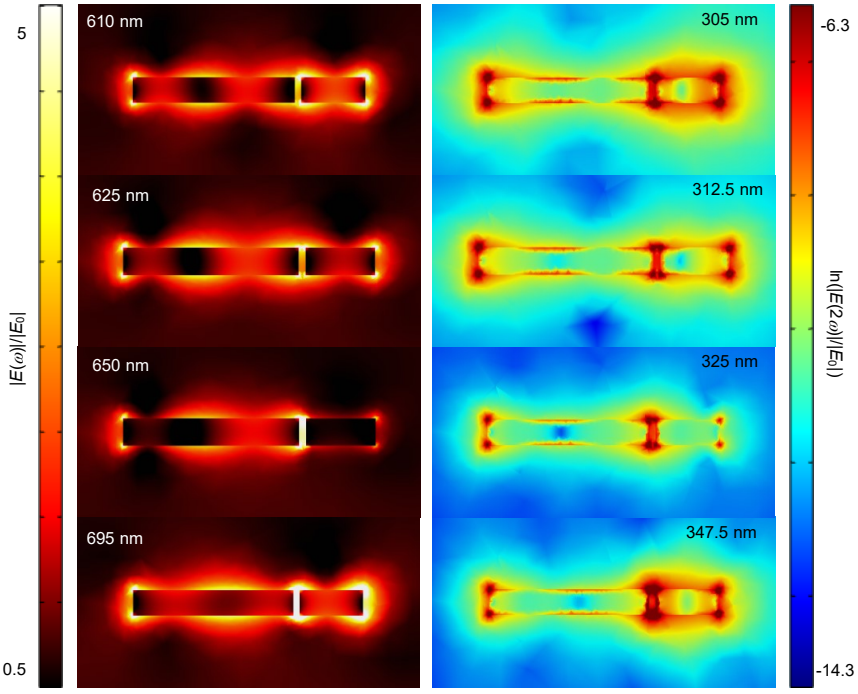

Fig. S14 The electric near field distributions at the fundamental (left) frequency of 610 nm, 625 nm, 650 nm, 695 nm and the electric near field distributions at the second harmonic (right) frequency of 305 nm, 312.5 nm, 325 nm, 347.5 nm.

References

1 M. Yorulmaz, A. Hoggard, H. Zhao, F. Wen, W. S. Chang, N. J. Halas, P. Nordlander and S. Link, *Nano Lett.*, 2016, DOI: 10.1021/acs.nanolett.6b03080.

2 Z. Fang, Y. Wang, Z. Liu, A. Schlather, P. M. Ajayan, F. H. Koppens, P. Nordlander and N. J. Halas, *ACS Nano*, 2012, **6**, 10222.

3 M. W. Knight, H. Sobhani, P. Nordlander and N. J. Halas, *Science*, 2011, **332**, 702.